JOURNAL OF GEOPHYSICAL RESEARCH, VOL. 111, C12005, doi:10.1029/2006JC003715, 2006

Trajectory prediction using HF radar surface currents: Monte Carlo simulations of prediction uncertainties

David S. Ullman,[1] James O'Donnell,[2] Josh Kohut,[3] Todd Fake,[2] and Arthur Allen[4]

Received 18 May 2006; accepted 15 August 2006; published 8 December 2006.

[1] An important aspect of particle trajectory modeling in the ocean is the assessment of the uncertainty in the final particle position. Monte Carlo particle trajectory simulations using surface currents derived from standard-range and long-range CODAR HF radar systems were performed using random-walk and random-flight models of the unresolved velocities. Velocity statistics for these models were derived from the covariance functions of differences between CODAR and drifter estimates of surface currents. Comparison of predicted trajectories and drifter tracks demonstrate that these predictions are superior to assuming the drifters stay at their initial position. Vertical shear between the effective depth of long-range CODAR measurements ($\sim$2.4 m) and that of drifters (0.65 m) causes the drifters to move more rapidly downwind than predicted. This bias is absent when standard-range CODAR currents (effective depth $\sim$0.5 m) are used, implying that drifter leeway is not the cause of the bias. Particle trajectories were computed using CODAR data and the random-flight model for 24-hour intervals using a Monte Carlo approach to determine the 95% confidence interval of position predictions. Between 80% and 90% of real drifters were located within the predicted confidence interval, in reasonable agreement with the expected 95% success rate. In contrast, predictions using the random-walk approach proved inconsistent with observations unless the diffusion coefficient was increased to approximately the random-flight value. The consistency of the random-flight uncertainty estimates and drifter data supports the use of our methodology for estimating model parameters from drifter-CODAR velocity differences.

Citation: Ullman, D. S., J. O'Donnell, J. Kohut, T. Fake, and A. Allen (2006), Trajectory prediction using HF radar surface currents: Monte Carlo simulations of prediction uncertainties, *J. Geophys. Res.*, *111*, C12005, doi:10.1029/2006JC003715.

1. Introduction

[2] Accurate prediction of Lagrangian trajectories in the coastal ocean is valuable to search and rescue (SAR) operations as well as for improving our understanding of how physical processes influence coastal ecosystems. The SAR challenge is to make a prediction of the path of a drifting search target given estimates of an initial location and the evolution of the velocity field. In addition, it is essential that the statistics of the prediction uncertainties be provided so that search planners can use available assets most effectively.

[3] Understanding the role of circulation variability in the coastal ocean on the recruitment of benthic species with pelagic larval stages poses a related ecological question [see, e.g., *James et al.*, 2002]. Given a source area and an Eulerian description of the circulation, what are the trajectories of larvae and how do the uncertainties in measurements and unresolved motions determine the statistics of the dispersion? Coastal radars and numerical models can provide estimates of the evolution of the velocity field, however, the dispersion or spread of particles, the uncertainty region in the SAR example, is more difficult to specify.

[4] The recent proliferation of coastal high frequency (HF) surface wave radar installations for mapping surface ocean currents provides a rapidly expanding capability for near real-time observation of surface currents. These data have the potential to dramatically improve the efficiency and success rate of SAR operations in coastal waters. For this reason, the U.S. Coast Guard (USCG) Research and Development Center has initiated a program to assess the effectiveness of trajectory predictions using currents derived from HF radar, and if warranted to implement the use of this technology on an operational basis. Preliminary work toward this end was reported by *Ullman et al.* [2003] and *O'Donnell et al.* [2005].

[5] Trajectory modeling applied for SAR operations must provide a measure of the uncertainty in the surface current portion of drift of the SAR object in order for an optimal search area to be delineated. The search area is a compromise between the need to define a large enough area to ensure that it encloses the target and the fact that search

[1]Graduate School of Oceanography, University of Rhode Island, Narragansett, Rhode Island, USA.
[2]Department of Marine Sciences, University of Connecticut, Groton, Connecticut, USA.
[3]Institute of Marine and Coastal Studies, Rutgers University, New Brunswick, New Jersey, USA.
[4]U.S. Coast Guard Office of Search and Rescue, Groton, Connecticut, USA.

0148-0227/06/2006JC003715$09.00

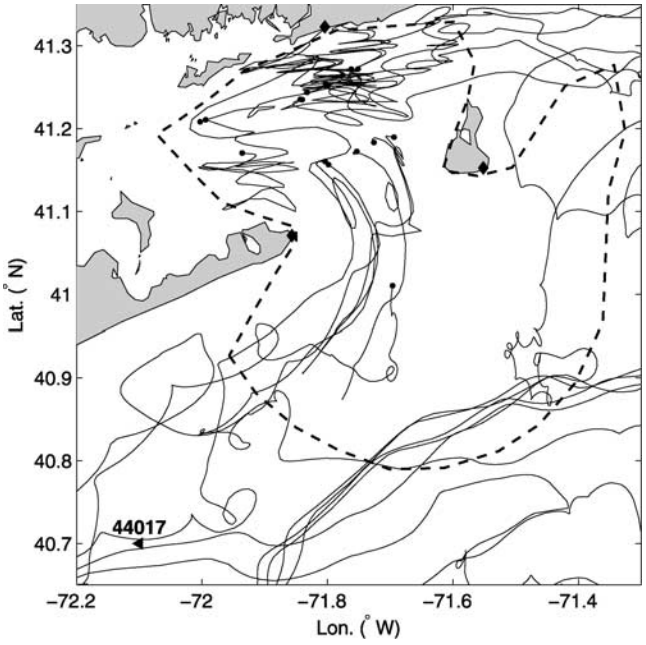

Figure 1. Trajectories of surface drifters deployed during December 2002 and March 2003 in the BI CODAR region. The black dots show the release points of each drifter (note that some were retrieved and redeployed). The black diamonds show the locations of the CODAR sites and the dashed line shows the approximate 10% coverage region. The location of NDBC buoy 44017 is denoted by the triangle.

resources are finite. The size of an operational search area is related to the magnitude of various uncertainties including those introduced by poorly known initial target position and time, velocity errors, and target leeway.

[6] The main objective of this paper is to evaluate a methodology for estimating uncertainty regions for simulated particle trajectories. The focus is on the uncertainty region, or search area in SAR terminology, due only to uncertainties in the drifter advective velocity provided by HF radar systems. The velocity uncertainties are modeled as a stochastic component representing a combination of unresolved or subgrid-scale motion and errors in the HF radar velocity retrieval. The parameters describing the stochastic variability are determined using a comparison of radar velocities and velocities of all available drifters passing through the radar domain. A secondary focus is the evaluation of the accuracy of trajectory predictions simulated using HF radar currents. Although the motivation of the project was the improvement of SAR trajectory predictions, we believe that the methodology described here is also applicable to the general Lagrangian prediction problem.

[7] Uncertainty regions are estimated using a Monte-Carlo approach whereby the trajectories of an ensemble of 1000 particles are simulated for 24-hour intervals. The Eulerian velocity is decomposed into a deterministic, large-scale component measured by the radar plus a stochastic component representing a combination of subgrid-scale motion and errors in the radar velocity. To simulate the Lagrangian motion, we make use of the hierarchy of particle trajectory models outlined by *Griffa* [1996], in particular the random-walk and random-flight models.

2. Data Sources

2.1. Drifter Trajectories

[8] A number of drifter releases in the mid-Atlantic Bight were performed by the U.S. Coast Guard Research and Development Center over the period 2002–2004 with the objective of providing a data set with which to assess trajectory predictions. Drifters were released in Block Island Sound within the coverage region of the standard-range CODAR system operated by the Universities of Rhode Island and Connecticut (Figure 1). Some of these drifters eventually passed through the coverage region of Rutgers University's long-range CODAR system and a number of additional drifters were released within that zone as well (Figure 2).

[9] Drifters were deployed in December 2002 in the Block Island (BI) region and again in March 2003. A subset of the latter group subsequently moved southwest on the shelf and passed through the New Jersey (NJ) shelf CODAR coverage region. A deployment of drifters was also made in March 2003 within the NJ shelf domain. A final set of deployments was made during July 2004 in both regions, however the drifters released in the BI region rapidly exited that domain and did not provide useful trajectory segments. Table 1 summarizes the drifter deployments. Separate analyses are presented for each of three drifter data sets: (1) drifters within the BI region during winter-spring 2002–2003, (2) drifters within the NJ shelf region during early spring 2003, and (3) those within the latter region during summer of 2004.

[10] The drifters employed were self-locating datum marker buoys (SLDMB) which are a USCG operational version of the Coastal Ocean Dynamics Experiment (CODE) drifter [*Davis*, 1985]. The physical dimensions of the SLDMB are identical to those of a CODE drifter except that the height of the drag vanes is reduced from 1.0 m to 0.7 m [*Allen*, 1996]. The center of the drag vanes is located at a depth of 0.65 m, which is assumed to be the effective depth of a velocity estimate from the drifter. The drifters recorded Global Positioning System (GPS) fixes at ½ hour intervals and the fixes were transmitted to shore via the Argos communications network. With ½ hour sampling and a nominal GPS position uncertainty of 10 m, the uncertainty in the velocity of the drifter due to position uncertainty is O(1 cm/s). *Davis* [1985] concluded, from comparisons of drifter velocities with near-surface vector measuring current meters, that the drifter velocity is accurate to approximately 3 cm/s. More recent measurements, using small current meters mounted within either end of the body tube of a CODE drifter, indicate that drifter slippage relative to the water is in the range of 2–5 cm/s (P. Poulain, personal communication, 2005).

2.2. HF Radar Surface Currents

[11] HF radar surface currents were obtained with CODAR SeaSonde systems located in the mid-Atlantic Bight in the region around Block Island and on the shelf east of New Jersey. A 3-site standard-range (~25 MHz)

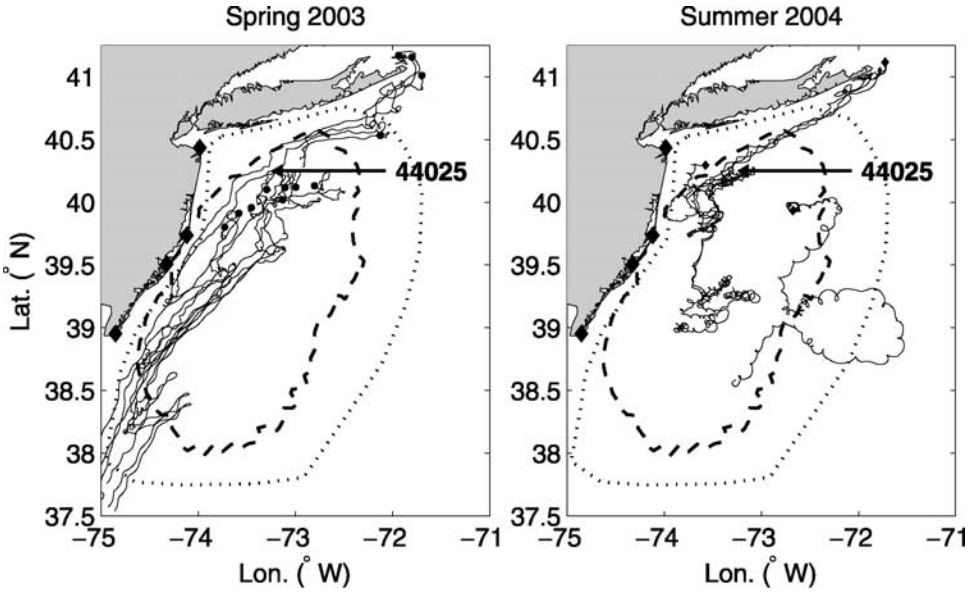

Figure 2. Trajectories of surface drifters deployed during March 2003 (left) and July 2004 (right) which passed through the NJ shelf CODAR domain. The black dots show the release points of each drifter. The black diamonds show the locations of the CODAR sites. The dotted line shows the nominal coverage zone, and the dashed line shows the approximate 10% coverage region. The location of NDBC buoy 44025 is indicated by the arrow.

system in the BI region provided hourly surface currents at 1.5 km resolution over the region shown in Figure 1. Radial velocities observed at each of the 3 sites were obtained with the MUltiple SIgnal Classification (MUSIC) algorithm [*Schmidt*, 1986] using measured antenna patterns. The radial components were combined to produce vector velocities using the manufacturer's (CODAR Ocean Sensors) software. The NJ shelf surface currents were provided by a 4-site long-range (~5 MHz) system with spatial resolution of 6 km in the area shown in Figure 2. Radial velocities averaged over 3-hour periods, estimated using measured antenna patterns, were output on an hourly basis and were combined using the Naval Postgraduate School's HF Radar Toolbox. A screening methodology, utilizing a threshold on the estimated geometric dilution of precision (GDOP) [*Gurgel*, 1994], was used to remove current vectors derived from combinations of radials with poor geometry. The GDOP, a nondimensional scalar was calculated for every grid point in the field at each time step. Larger GDOP values indicate poor geometry in which the available radial component vectors do not adequately resolve both components of the current. For the analysis in this paper, an empirically determined threshold of 1.25 was used, whereby vectors for which the GDOP was greater than the threshold were eliminated from consideration.

[12] HF radar estimation of surface currents relies on Bragg scattering from surface gravity waves having a wavelength exactly ½ the radar wavelength and traveling either towards or away from the radar site [*Stewart and Joy*, 1974]. The backscattered signal is Doppler shifted by an amount proportional to the sum of the wave phase velocity, which is known via the deep-water dispersion relation, and the radial component of the surface current upon which the Bragg waves are carried. The surface current is then the difference between the velocity of the Bragg waves estimated from the measured Doppler shift and the computed phase velocity. The effective depth of the surface current measurement depends on the wavelength of the Bragg waves, and thus on the radar frequency. *Stewart and Joy* [1974] showed that, for a linear surface current vertical profile, the effective measurement depth is given by:

$$d_{eff} = \frac{\lambda_{bragg}}{4\pi} = \frac{\lambda_{radar}}{8\pi} \tag{1}$$

Using this equation, the effective depths of the current measurements are estimated to be ~0.5 m for the 25 MHz standard range system in the BI region, and ~2.4 m for the 5 MHz long range system along the NJ coast.

[13] Estimates of the uncertainties associated with surface currents derived from CODAR systems have been provided using in situ velocity observations from acoustic Doppler current profilers (ADCPs). *Chapman and Graber* [1997] cite differences of O(15 cm/s) between HF radar current estimates and in situ current measurements. However, as *Kohut et al.* [2006] point out, these error estimates include a large component that is due to the different spatial scales and depths sampled by HF radar and ADCPs. They estimate the intrinsic CODAR radial uncertainty to be of O(5 cm/s)

Table 1. U.S. Coast Guard Research and Development Center Mid-Atlantic Bight Drifter Releases During 2002–2004

Date	Region	Number	Notes
16–18 Dec 2002	BI	9	Retrieved and redeployed several.
27 Mar 2003	BI	4	Passed through NJ Shelf region.
27 Mar 2003	NJ Shelf	8	
27 Jul 2004	BI	3	Rapidly left domain.
			Passed through NJ Shelf region.
27 Jul 2004	NJ Shelf	4	

for the NJ shelf long-range systems used in the present study. Vector uncertainties for the BI region were estimated to be 3–15 cm/s with the larger values observed along the outer boundaries of the coverage regions where the combining geometry is nonoptimal and where signal to noise ratios increase [*Ullman and Codiga*, 2004].

[14] Interpolation of velocities from the CODAR grid to the location of a drifter was performed using a weighted, nearest neighbor scheme in which velocities from the 4 nearest neighbor grid points were weighted inversely with distance. This method is more robust than bi-linear interpolation because it tolerates some data gaps and allows for extrapolation beyond the instantaneous zone of CODAR coverage if desired. In our analysis, we restrict the trajectory prediction evaluation to those drifter tracks that start within the nominal coverage zones shown in Figures 1 and 2. There is, however, variability in the extent of the area within which long range CODAR data is available and Figure 2 also shows where current estimates are available at least 10% of the time during the drifter deployment periods. Note that in the BI region the 10% coverage region and the nominal coverage region were the same. The 10% coverage regions were used to perform more stringent screening of the trajectories, confining them to regions of more reliable CODAR currents.

2.3. Comparison of Surface Currents From Radar and Drifters

[15] Drifter velocities at times (hourly) corresponding to CODAR observations were computed from time series of drifter positions at half-hour intervals using a central difference scheme. CODAR velocities were then spatially interpolated to the drifter location using the weighted nearest neighbor method described above. Velocities at locations outside of the 10% coverage zones (see Figures 1 and 2) were eliminated from the analysis.

[16] Velocity differences (drifter minus CODAR) were rotated into a right-handed coordinate system with x oriented in the direction of the instantaneous wind and y oriented in the cross-wind direction. Hourly wind measurements from National Data Buoy Center buoys 44017 and 44025 were used for the BI and NJ shelf regions respectively (see Figures 1 and 2 for the location of these buoys). Winds were assumed to be spatially uniform over each of the CODAR domains. In the NJ shelf region, downwind drifter-CODAR differences are weakly correlated (r = 0.28) with wind speed indicating a tendency for the drifters to move faster downwind than the CODAR measurements (Figure 3a). The correlation is significantly different from zero assuming N/24 degrees of freedom, where N = 5895 is the number of hourly data points in Figure 3a and the factor 24 is the estimated integral timescale in hours of the wind speed (not shown). In the BI region, downwind drifter-CODAR differences are uncorrelated with the wind speed, and crosswind differences are uncorrelated in both regions (Figure 3).

[17] The effective depth of the 25 MHz BI region CODAR ($\sim$0.5 m) is very close to the effective depth of the drifters ($\sim$0.65 m). The lack of correlation between downwind drifter-CODAR difference and wind speed in this case suggests that drifter leeway is indeed small. The positive correlation exhibited in the NJ shelf region with long-range CODAR measurements at $\sim$5 MHz is consistent with the presence of vertical shear between the drifter depth and the effective depth of the CODAR measurement (2.4 m). To demonstrate this, we estimated the vertical shear between the drifter and CODAR effective depths as a superposition of a steady-state Ekman spiral and the Stokes drift. Ekman currents were computed using a constant eddy viscosity of 10^{-2} m^2/s at 40° N and the Large and Pond drag coefficient formulation [*Large and Pond*, 1981]. The Stokes drift was estimated using the *Pierson and Moskowitz* [1964] n = 4 spectrum for a fully developed wave field following *Kenyon* [1969]. To simplify the calculation, angular spreading of the energy spectrum was neglected. The estimated velocity difference between z = 0.65 m and z = 2.4 m from the combined Ekman and Stokes currents is plotted in Figure 3a as a function of wind speed (green line). Although the scatter is large, the estimated difference appears to explain the general trend, suggesting that the correlation between drifter-CODAR differences and wind speed arises due to vertical shear between the depths of the drifter and the CODAR measurements.

3. Trajectory Modeling

3.1. Monte-Carlo Trajectory Prediction

[18] The motion of a particle in a two-dimensional velocity field can be described by the equation:

$$\frac{d\boldsymbol{r}}{dt} = \boldsymbol{u}(t, \boldsymbol{r}), \tag{2}$$

where $\boldsymbol{r} = (x, y)$ denotes the position of the particle and $\boldsymbol{u} = (u, v)$ is the Eulerian velocity at position $\boldsymbol{r}$ and time t. The velocity can be decomposed into a large-scale, slowly varying component $\boldsymbol{U}$, and a component $\boldsymbol{u_t}$ representing subgrid-scale deviations which will be referred to as turbulence:

$$\boldsymbol{u} = \boldsymbol{U} + \boldsymbol{u}_t. \tag{3}$$

Surface current mapping radars such as CODAR can provide estimates of $\boldsymbol{U}$ at spatial scales of approximately 1.5 km (6 km) and temporal scales of 1 hour (3 hours) for standard-range (long-range) systems, thus the turbulent component represents velocity fluctuations on scales smaller than these. The radar-derived velocity is subject to significant uncertainties and so the large-scale component can be expressed as:

$$\mathbf{U} = \mathbf{U}_{radar} + \delta\mathbf{u}, \tag{4}$$

where $\boldsymbol{U_{radar}}$ is the radar measurement and $\delta\boldsymbol{u}$ is the measurement error. Combining (3) and (4), the total Eulerian velocity can be written:

$$\boldsymbol{u} = \boldsymbol{U}_{radar} + \boldsymbol{u}_t + \delta\boldsymbol{u} = \boldsymbol{U}_{radar} + \boldsymbol{u}', \tag{5}$$

where $\boldsymbol{u}'$ includes both the turbulent velocity and the measurement error.

[19] Prediction of particle trajectories in a region of HF radar coverage was achieved by integrating (2) using a predictor-corrector scheme with the velocity given by (5).

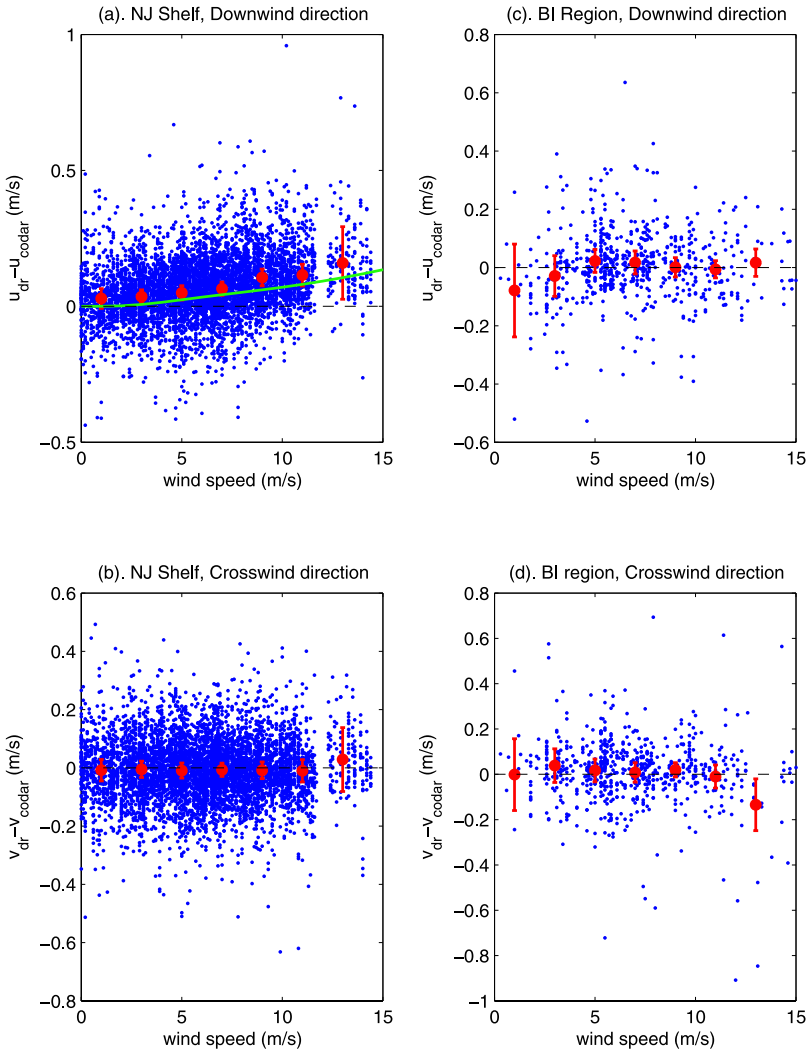

Figure 3. Differences between drifter and CODAR velocity resolved into the downwind and crosswind directions versus wind speed for drifters in (a, b) the NJ shelf region and (c, d) the BI region. Wind data are from NDBC buoy 44025 for the NJ shelf comparisons and buoy 44017 for the BI comparisons. The red circles are mean differences within 2 m/s wind speed bins. The error bars on the means are at the 95% level, computed using a *t*-test with N/24 degrees of freedom, where N is the number of hourly values in the bin and 24 hours is the approximate integral timescale of the wind speed. The green line in Figure 3a is an estimate of the shear between the effective depths of the drifter (0.65 m) and the long-range CODAR (2.4 m) due to the sum of the Ekman component and the Stokes drift.

A time-step of 1 hour was used and radar velocities were interpolated to the particle location using the weighted nearest neighbor approach. The methodology for specifying $\boldsymbol{u}'$ is described in the following section.

3.2. Subgrid-Scale Velocity Model

[20] Although $\boldsymbol{u}'$ is a combination of radar measurement errors, unresolved motion, and true geophysical turbulent fluctuations, we assume that its properties can be described by models that have been used to describe turbulence alone. We are somewhat compelled to combine the components of $\boldsymbol{u}'$ as there is no simple way to separate them. However, since drifters are now routinely launched during U.S. Coast Guard SAR operations and coastal current radar systems are proliferating, there is potentially substantial value in a methodology that allows the estimation of the statistics of $\boldsymbol{u}'$ from comparison of drifter and radar velocities. The assumption that the properties of $\boldsymbol{u}'$ can be described by models of turbulence will be shown in the following to yield predictions that are consistent with observations.

[21] Two models of turbulence (by which we mean $\boldsymbol{u}'$) were examined. Both are members of the hierarchy of stochastic particle models reviewed by *Griffa* [1996] and assume that the two horizontal components are independent. The so-called random-walk and random-flight models both assume that the particle position is Markovian. The latter also assumes that the particle velocity is a Markovian variable. Physically, the random-flight model recognizes that the turbulent velocity fluctuations have a finite temporal correlation scale whereas the random-walk model assumes that the correlation scale is infinitesimal. When the same turbulent velocity variance is used in the two models, one

expects greater particle dispersion with the random-flight version.

[22] The random-walk formulation for the components of $\boldsymbol{u}'$ (u' and v') can be expressed as:

$$u' = \sigma_u \frac{T_u^{1/2}}{dt} \cdot dw, \tag{6}$$

where σ_u is the velocity standard deviation and dw is a normally distributed random increment with zero mean and second moment $\langle dw \cdot dw \rangle = 2 \cdot dt$ where dt the time step for the integration of (2). Note that the turbulent timescale T_u in the discrete problem is not actually infinitesimal but is constrained to equal $dt/2$ to obtain consistency between (6) and the definition of velocity variance [*Griffa*, 1996].

[23] The evolution of the turbulent velocity in the random-flight turbulence model is described by:

$$du' = -\frac{u'}{T_u} dt + \frac{\sigma_u}{T_u^{1/2}} dw. \tag{7}$$

The first term on the right of (7) introduces "memory" with a timescale T_u to the model of the turbulent fluctuations and the second term is, as in the random-walk model, a random impulse. As is easily demonstrated, the autocorrelation function of the u' in (7) decays exponentially with an e-folding time, or integral timescale, equal to T_u [*Griffa*, 1996].

[24] It is important to note that the diffusion coefficient for particles in homogeneous turbulence at times large compared with T_u is defined as:

$$K_x = \sigma_u^2 \cdot T_u \tag{8}$$

[*Csanady*, 1973]. Since for the random-walk case, $T_u = dt/2$, the dispersion for a specified σ^2 is dependent on the time step employed in the numerical implementation of this model.

3.3. Estimating Turbulent Velocity Statistics

[25] Practical implementation of the aforementioned turbulence models to determine the random velocity components in (5) requires specification of the velocity variance σ^2, and, for the random-flight case, the turbulent timescale T. If the tracks of clusters of drifters, released simultaneously at a variety of locations were available, one could estimate the dispersion coefficient K and compute σ^2 and T if necessary. However, few such deployments have been undertaken. Much more frequently, a few drifters are deployed as part of a SAR operation. We propose an approach to exploit the drifter data obtained from this type of deployment, in conjunction with HF radar derived surface currents to estimate the fluctuating velocity statistics directly. From (5), the fluctuating velocity is:

$$\boldsymbol{u}' = \boldsymbol{u} - \boldsymbol{U}_{radar}.$$

Although clearly, the true velocity $\boldsymbol{u}$ is not known, we argue that the drifter velocity is our best estimate of it and is the natural choice especially for SAR applications. Previous work suggests that the leeway associated with CODE-type drifters is small, and further support for this result is provided by Figure 3c, which shows no discernable relation between downwind drifter-CODAR velocity difference and wind speed for the case where the effective depth of drifter and CODAR are equal. The positive relationship found for drifter-CODAR differences in the NJ shelf long-range CODAR domain are associated with the difference in effective depth of the two velocity measurements. Even in this region, other sources of errors clearly dominate the observed differences. Moreover, if the objective is to predict the motion of a drifting object at the surface, it seems eminently sensible to take the drifter velocity as the true velocity.

[26] Time series of $\boldsymbol{u}'$ for each drifter, the difference of the drifter and the interpolated CODAR velocities, were used to compute autocovariance functions for the u' and v' components. These were subsequently averaged over all drifter tracks to produce the curves shown in Figure 4. The autocovariance functions for both the BI and NJ shelf regions exhibit rapid decay at lags of several hours. Low amplitude periodicities at the semi-diurnal period are evident in the BI region and in a broad band around the inertial period in the NJ shelf region during 2004 (Figure 4). The cross-covariances (not shown) are generally low, consistent with the assumption that the horizontal velocity components fluctuate independently. We estimate the turbulent variances as the zero-lag values of the autocovariance functions for each deployment. Turbulent integral timescales for the two velocity components were estimated by fitting exponential autocovariance functions to the observed autocovariances at lags of 1 and 2 hours. Although computationally much simpler than the method of moments technique used by *Griffa et al.* [1995], this method is similar to theirs in that only autocovariances at short lags, which are statistically most reliable, are used to estimate the turbulent timescale. The best fit exponential autocovariance functions are shown as dashed curves in Figure 4 and the parameter estimates are given in Table 2. Integral timescales are approximately 1.5 hours in the BI region and 3–5 hours in the NJ shelf region, with higher values during the spring 2003 deployment in the latter region.

3.4. Sensitivity to Number of Particles and Time Step

[27] It is well known that the results of stochastic particle modeling can be sensitive to the particular details of the methodology used [e.g., *Brickman and Smith*, 2002]. One of the most important methodological parameters in the simulation of particle dispersion is the number of trials (particles) simulated. If too few particles are used, the estimate of dispersion will have a large uncertainty, while a simulation with too many particles can be computationally costly. To investigate the sensitivity of dispersion estimates on the number of simulated particles, we performed a 24-hour, 10,000-particle simulation using the random-flight model with zero large-scale flow. From the 10,000 particle trajectories, we randomly subsampled 100 ensembles of N particles, with N ranging from 100 to 5000 particles. The variance of final particle position was computed for each ensemble and was compared with the analytical solution given by *Griffa* [1996]. Figure 5 shows that as the number of particles increases, the potential error in the estimated dispersion decreases. With 100 particles, the error in dispersion can be

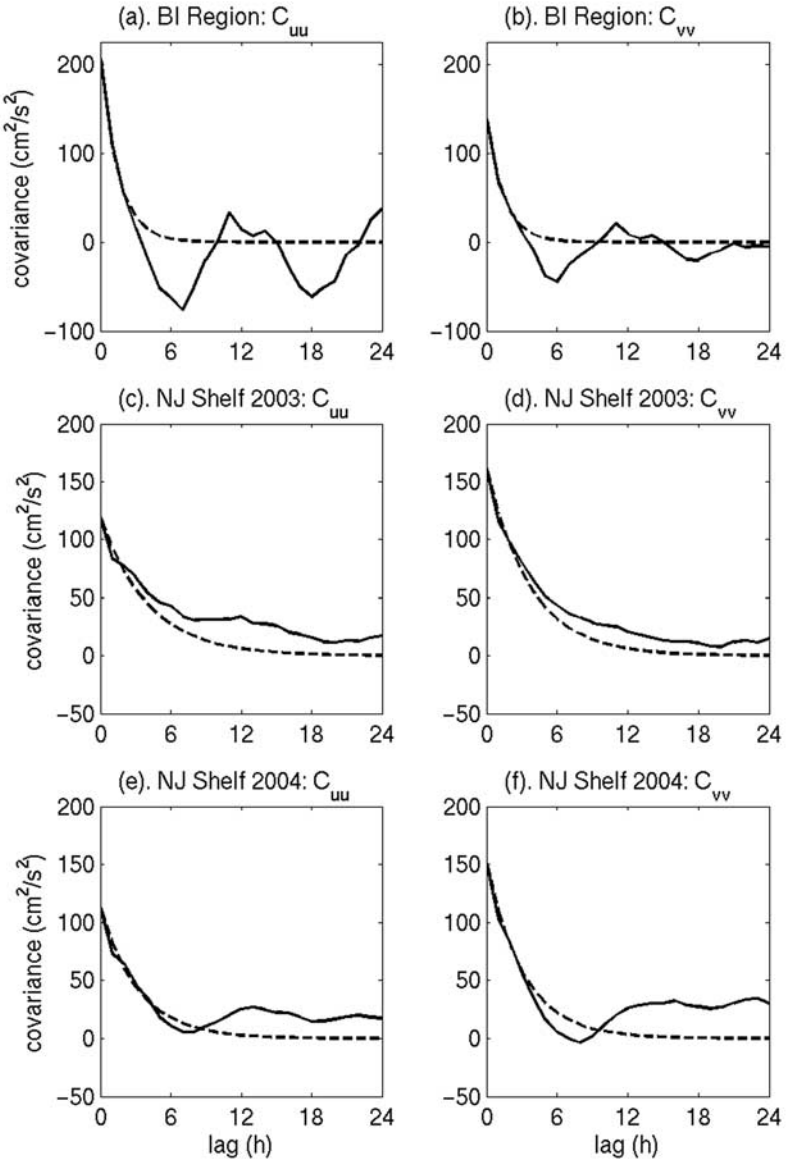

Figure 4. Lagged autocovariance functions of time series of differences between drifter velocity and CODAR velocity averaged over all drifters within the BI region for (a) the eastward component and (b) the northward component. The solid curves are the computed autocovariance functions, and the dashed lines are the best fit exponential covariance functions. Covariance functions for the NJ shelf region (c, d) during 2003 and (e, f) for 2004.

up to 5–6 km^2, whereas the use of 5000 particles reduces the expected error to less than ~1 km^2. In order to reduce the computational load, we used 1000 particles for the results presented in section 4, in which case the error in dispersion is at most ~2 km^2.

[28] Although the CODAR currents are produced on an hourly basis, we nonetheless investigated the sensitivity of the dispersion estimates to the time step of the particle advection scheme. The CODAR velocities within the BI region were interpolated in time to ½ hour intervals and the random-walk and random-flight simulations performed using a ½ hour time step in the integration. The turbulent velocity statistics were as given in Table 2. Although not shown here, we found that the dispersion, and thus the search areas, for the random-flight case were essentially unchanged from the results using a 1-hour time step. The random-walk results, as noted above in section 3.2, are expected to depend on the time step, and indeed we found reduced dispersion occurring for the case of dt = 0.5 h. However, the conclusions we reach, in section 4.2, regarding the relative merits of the random-walk and random-flight methods using a 1-hour time step would not have changed had we performed the simulations using a reduced time step.

4. Results

[29] To evaluate our approach to modeling dispersion and to the estimation of parameters, we compared observed drifter trajectories to those predicted retrospectively using

Table 2. Estimates of Random-Flight Turbulence Parameters From Least Squares Fits to the Autocovariance Functions of Drifter-CODAR Velocity Differences for the Three Drifter Deployments

Region	σ_u, m/s	T_u, h	K_x, m^2/s	σ_v, m/s	T_v, h	K_y, m^2/s
BI (2003)	0.14	1.5	106	0.12	1.4	73
NJ Shelf (2003)	0.11	4.1	179	0.13	3.7	225
NJ Shelf (2004)	0.11	3.3	144	0.12	3.1	161

CODAR velocities. Each drifter trajectory was divided into 24-hour segments with each segment overlapping the previous one by 12 hours for drifters within the BI region. Example simulations are shown in Figure 6 together with the 95th percentile confidence regions for the final pseudo-drifter location (the gray polygons). To define the confidence interval, we first computed the two-dimensional frequency histogram of the terminal pseudo-drifter locations and then rank ordered the spatial bins by frequency. Proceeding from the most to the least frequent, bins were included in the confidence interval and shaded gray until 95% of the total number of simulations (1000) was included.

[30] In the analysis that follows, we present the statistics of the trajectory differences for all trajectories that begin within the area of CODAR coverage as well as for a subset with the end position also located within the coverage region. The number of trajectory comparisons versus the time since the start of the prediction is shown in Figure 7. The decrease with time in the BI region results from the retrieval and redeployment of drifters that left the CODAR domain; thus a number of "short" trajectories (<24 hours) is present in the trajectory ensemble.

4.1. Accuracy of Predictions

[31] The accuracy of a drifter trajectory prediction is measured by the distance between the real drifter and the pseudo-drifter. This was computed for each hour of each 24-hour trajectory segment. The ensemble mean separation and the 95th percentile separation are presented in Figures 8–10 for the three deployments. Mean separation generally increases with time in a linear fashion with some indication that separations at short times increase at a slightly faster rate. At 24 h, mean separation is approximately 7 km (6 km) for the BI unscreened (screened) ensembles (Figure 8). In the NJ shelf region, using the screened (unscreened) ensembles, 24-hour separations are 11 km (9 km) during the spring 2003 deployment (Figure 9) and 8 km (7 km) during the summer 2004 deployment (Figure 10). The 95th percentile separation values are also somewhat higher in the NJ shelf domain, especially during 2003, with 24-hour values for the unscreened subset reaching 25 km during 2003 and 20 km during 2004 compared to about 18 km for the BI drifters. When drifters leaving the CODAR region are screened from the analyses, the 95th percentile separations (24 hours) are about 17 km and 15 km for the 2003 and 2004 deployments in the NJ shelf region and 12 km in the BI region. The general decrease in error with screening is not surprising, and is consistent with the occurrence of relatively large trajectory prediction errors along the outer boundary of the CODAR domain where radar-derived velocity errors increase.

[32] To assess the value of the CODAR-based drifter predictions, we compare the performance to the simplest alternative prediction strategy, which is to assume that the drifter stays where it was initially released. The error in the so-called persistence, or last known position, forecast is simply the distance traveled by the drifter, and the mean and 95th percentile values are also shown in Figures 8–10. Drifters released in the BI region and during the 2003 shelf deployment tend to travel farther than those released on the shelf during summer 2004. Using the unscreened trajectories, the mean (95th percentile) distance traveled after 24 hours in the BI region is 15 km (38 km) compared with about 20 km (44 km) during 2003 and 11 km (23 km) during 2004 in the NJ shelf region. The net result is that drifter locations predicted using CODAR currents in the BI

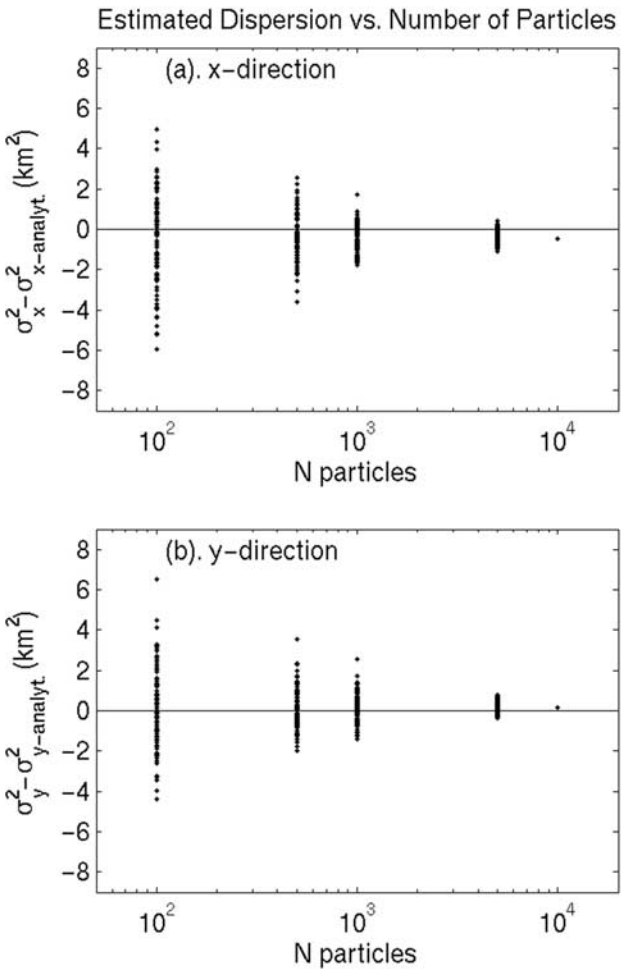

Figure 5. Variance in particle position in the (a) x-direction and (b) y-direction compared to the analytical solution for variance, as a function of the number of particles sampled. The simulation was performed using the random-flight turbulence model with $\sigma_u = \sigma_v = 10$ cm/s and $T_u = T_v = 3$ h.

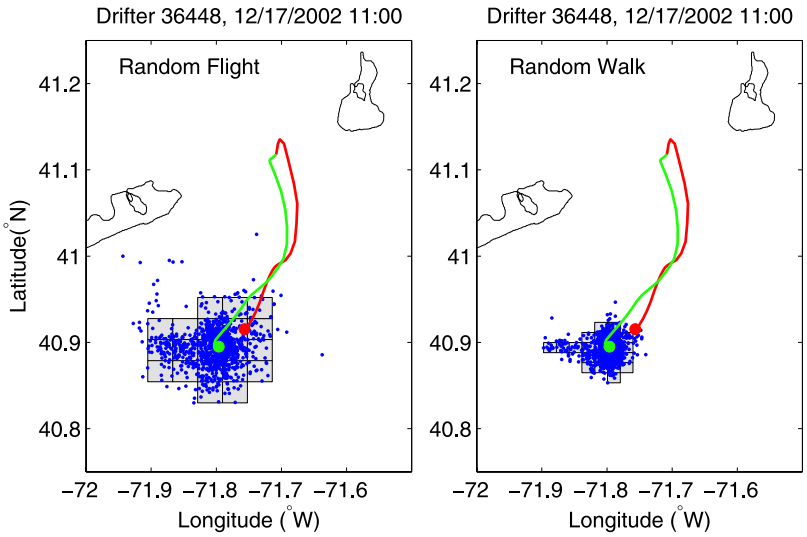

Figure 6. Example drifter trajectory within the BI CODAR region showing the real drifter path over 24 hours in red and the CODAR predicted position in green, with final positions denoted by the circles. The ensemble of trajectory prediction endpoints using the random-flight (left) and random-walk (right) models are shown as blue dots. The gray polygons denote the region within which 95% of the drifter final positions lie.

region are on average approximately 50% closer to the real drifter position than are the last known positions. This is also true for the NJ shelf deployment during 2003, but this effect is less pronounced on the shelf where the mean distance from the predicted position to the real drifter is about 70% of the distance traveled. Similar conclusions are reached using the screened drifter subsets, although the screening can be seen to sharply reduce the 95th percentile separation value in the BI region.

[33] The observed correlation between drifter-CODAR velocity differences and wind speed for the NJ shelf long-range CODAR (Figure 3a) suggests that the accuracy of predicted drifter positions should also be correlated with wind speed. For each trajectory, the mean eastward and northward wind components were computed over the entire 24-hour prediction time. The separation vector between the real and simulated positions at 24 hours was then rotated into a coordinate system oriented in the mean downwind and crosswind directions. For the NJ shelf drifters, Figure 11 shows that the downwind component is in fact correlated ($r = 0.49$, significant at the 95% level) with the magnitude of the vector-averaged wind. No such correlation is found for the drifters in the BI region (not shown), which is consistent with the lack of a relationship between wind and drifter-CODAR velocity differences in that region (Figure 3c).

4.2. Uncertainty Bounds for Predictions

[34] The Monte Carlo simulation of trajectories provides an ensemble of final drifter locations that are extremely valuable in the important practical problem of defining a search area. If we take the interval containing 95% of the pseudo-drifter positions computed using the random-walk and random-flight turbulence models as the search area, then it is important to know whether the real drifters (search targets) are found within this area at the expected frequency. At each hour of each drifter trajectory, the search area was computed as described at the beginning of this section and the position of the real drifter checked to see whether it was inside or outside the search area. The number of real drifters within the search area was summed for each hour and this quantity was then divided by the number of trajectories to compute the fraction inside the predicted search area (the percent success).

[35] Figures 12 and 13 compare the time evolution of the percentage of real drifters found inside the simulated search areas using the two turbulence models and shows clearly that the random-flight method is superior for all three drifter deployments whether the drifter tracks that exit the CODAR coverage area are screened or not. Without screening 70–90% of all random-flight derived search areas enclosed the real drifter position and there was little variation with time. Screening the drifter data increased the fraction by 5–10% yielding percent success in the range 80–90% for the BI and 2003 NJ shelf deployment, and 85–95% for the 2004 shelf deployment. In the BI region, there appears to be semi-diurnal variability in the percent success (Figure 12) which may be related to the presence of a significant semidiurnal signal in the autocovariance functions in this area (Figures 4a and 4b).

[36] In contrast, search areas estimated using the random-walk model of turbulence appear to be too small, with percent success, for the unscreened drifter subset, dropping from about 70–85% at a prediction time of 1 hour to 20–60% after 24 hours. As for the random-flight results, the comparison using the screened subset improves by about 5% at all prediction times. The discrepancy between the search areas produced using the two turbulence models is most apparent for the simulations on the NJ shelf (Figure 13).

5. Discussion

[37] Drifter positions predicted over 24 hours using CODAR surface currents are clearly superior to the persis-

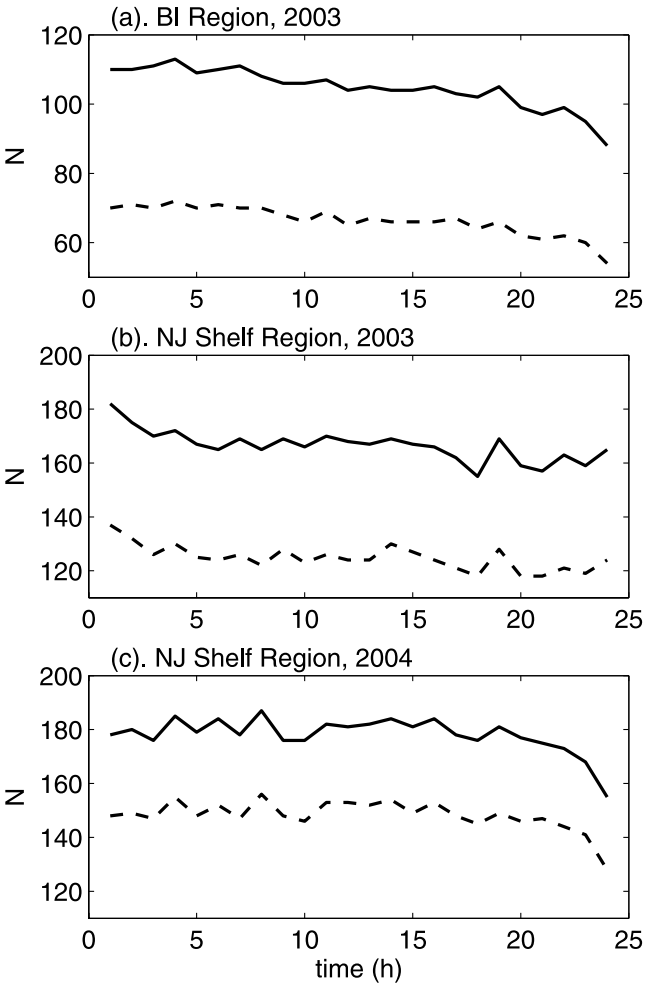

Figure 7. The number of comparisons between predicted and true drifter position versus time with no screening (solid lines) and with screening using the 10% coverage zone (dashed lines) for the (a) BI region, (b) NJ Shelf region during 2003, and (c) NJ Shelf region during 2004.

tence forecast in estimating the final drifter location. The mean separation between predicted and observed drifter location is 50–70% of the separation using the persistence forecast. Using currents from a numerical circulation model, *Thompson et al.* [2003] simulated the trajectories of a number of surface drifters on the Scotian Shelf. They estimated the 50th percentile separation value after 24 hours to be 6 km, which is very similar to the mean separation of 6–7 km found in the present study. This suggests that trajectory predictions using CODAR surface currents have comparable skill in predicting target trajectories as predictions using numerical model currents.

[38] Using long-range CODAR currents, trajectory predictions can be significantly in error under high-wind conditions. This appears to arise because of velocity shear between the effective measuring depths of the drifter (~0.65 m) and the CODAR (~2.4 m at 5 MHz). In this case, the real drifter experiences a greater wind-driven current in the direction of the wind. Such inaccuracies in trajectory predictions are not found when standard-range (25 MHz) CODAR currents (effective depth of ~0.65 m) are used for predictions. This suggests that, for SAR operations, it is important to utilize near-surface current data from a depth that is comparable to the effective depth of the drifting object. The correspondence, seen in Figure 3a,

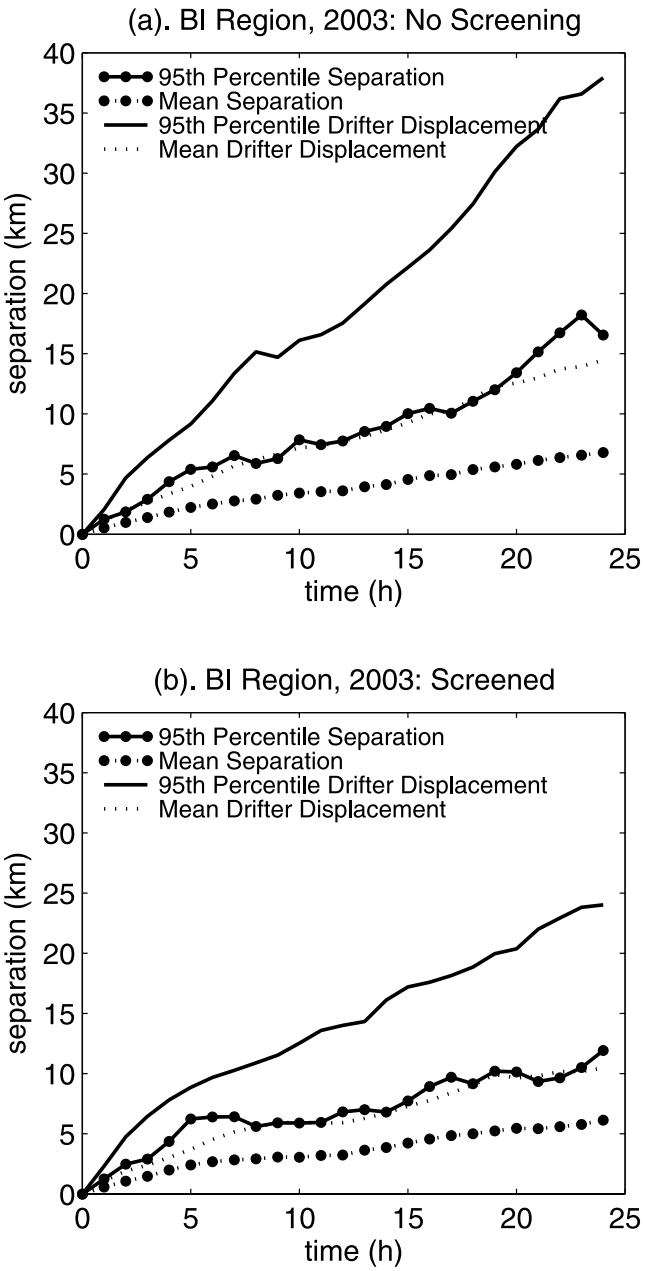

Figure 8. (a) Separation between actual and predicted drifter position as a function of time since start of prediction, averaged over all trajectory segments that start within the nominal coverage zone for the BI region. The curves with symbols show the mean separation (dashed line and circles) and the 95th percentile separation (solid line and circles) between the real drifter and the predicted position. The dashed and solid lines show respectively the mean distance and the 95th percentile distance that the real drifter moved over the prediction time. (b) The same statistical measures averaged over all segments that both start and end within the 10% coverage zone.

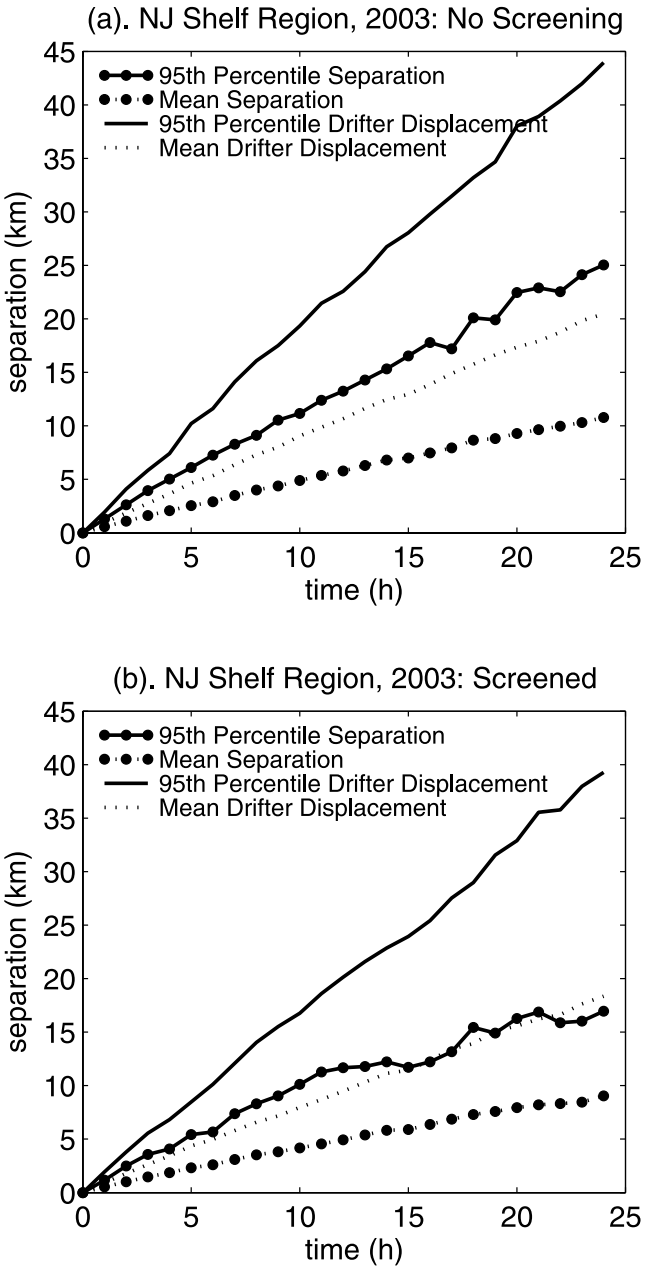

Figure 9. Same as Figure 8, but for the NJ shelf region during 2003.

between the predicted difference in velocity from 0.65 to 2.4 m and the observed drifter-CODAR differences indicates the possibility of correcting observed CODAR velocities to drifter depths if simultaneous wind data are available.

[39] The search area evaluations can be used to assess the consistency of the turbulence models and their associated parameters. A consistent turbulence model would be expected to provide, for instance, a 95% confidence region that is successful (with the real drifter location within it) 95% of the time. The random-flight method provides search areas that enclose the real drifter approximately 90% of the time, whereas the random-walk formulation does significantly worse. This suggests that, with the parameter(s) estimated from the drifters, the random-flight model is nearly self-consistent while the random-walk model is definitely not. The difference between the random-flight success rate and the expected 95% suggests a slight underestimate of either the turbulent variance or the timescale. The latter seems the more likely candidate here, as we have estimated the turbulent timescale from a least squares fit to the observed autocovariance at short lags. Figure 4 shows that the empirical exponential functions generally underestimate the covariance at large time lags, suggesting an underestimate of the timescale. Note that evaluation of the integral timescale by integration of the autocovariance to infinite lags is problematic in the presence of the quasi-periodic motions evident in the covariance functions of Figure 4.

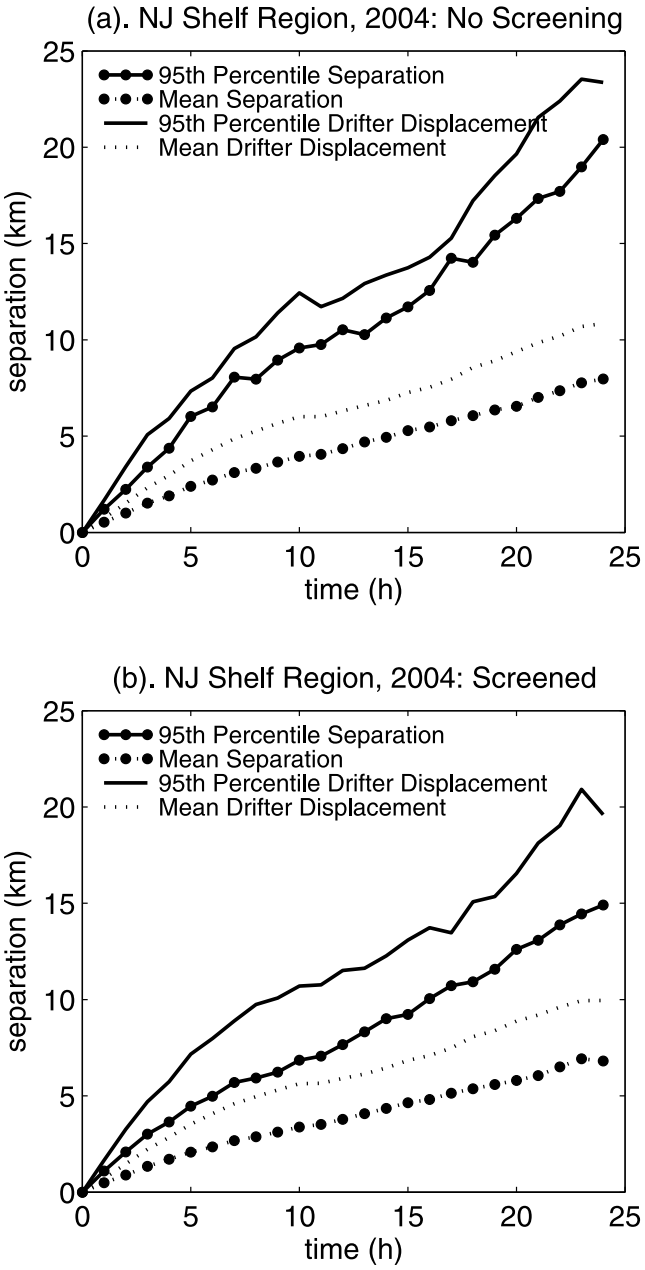

Figure 10. Same as Figure 8, but for the NJ shelf region during 2004.

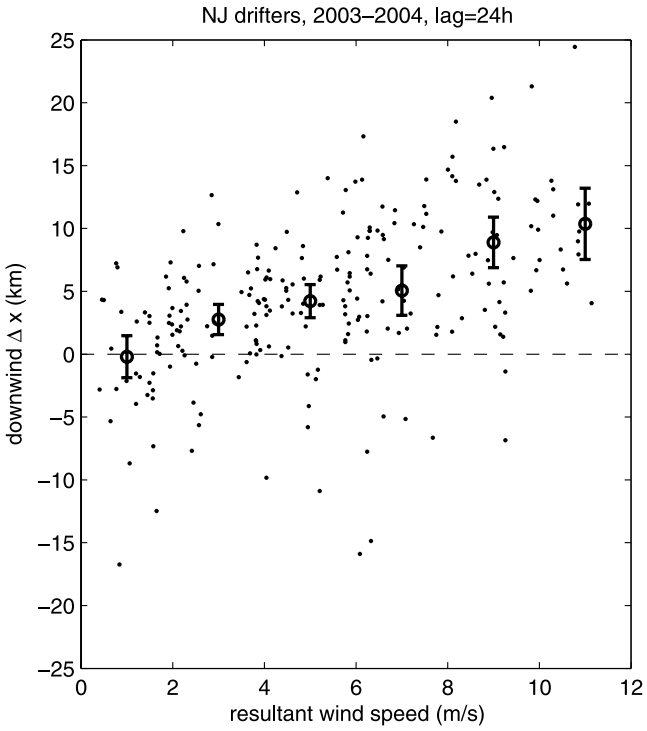

Figure 11. Downwind component of the difference in position between the real drifter position and the predicted position at 24 hours after the start of the prediction as a function of the vector mean wind speed over the 24-hour period for all drifters within the NJ shelf region. The dots denote individual trajectory segments, and the open circles represent the mean difference within 2 m/s bins. The error bars on the mean values are 95% confidence limits on the mean values estimated using a *t*-test.

[40] The wind speed bias observed in the NJ shelf region using long-range CODAR currents has a noticeable effect on search areas only near the end of the 24-hour prediction interval. A velocity bias Δv in the presence of diffusion will be negligible until such time, *t,* as the consequent error in displacement, $L_E = t\Delta v$, becomes of the order of the size of the diffusive particle cloud $L_D = \sqrt{Kt}$. For diffusivities of $\sim$200 m^2/s (Table 2) and velocity bias of $\sim$0.07 m/s (predicted velocity bias for 10 m/s wind), t is of order 11 hours. Examination of Figure 13a shows a gradual decrease in search area effectiveness at times greater than 15 hours for the 2003 NJ shelf drifters. Restricting the evaluation of the predicted search areas to cases of weak wind (<7 m/s) showed that search area effectiveness remained approximately uniform from 15 to 24 hours after the prediction start (not shown). This suggests that the gradual decrease in search area effectiveness observed in Figure 13a at large times is likely due to the inclusion of high-wind cases where the effect of the wind speed bias becomes noticeable.

[41] It is important to note that in the comparison of the effectiveness of random-walk and random-flight derived drifter dispersion the same turbulent velocity fluctuation variance (σ^2) has been used. If a larger value were chosen for the random-walk simulations then the search areas would be larger and the percent success consequently higher. If an estimate of the effective diffusivity ($\boldsymbol{K}$) were available and the fluctuation variances in both turbulence models and turbulent timescale in the random-flight model were chosen to be consistent with this value, the simulations of *Zambianchi and Griffa* [1994] show that the random-walk model overestimates the particle dispersion for $\boldsymbol{t < T_u}$ At times large compared to the turbulent timescale, the two models predict that the particle cloud size increases at the same rate, though the offset introduced by the initial overestimate persists. For turbulent timescales of 1–4 hours as determined in the present study, the difference is 10–20% at 12–24 hours after the start of the prediction.

[42] The result of increasing the random-walk diffusion coefficient to the random-flight value ($\boldsymbol{\sigma^2 T}$) for the 2004 NJ shelf deployment is demonstrated in Figure 14. In this case, search areas using the random-walk model are more effective in enclosing the real drifter position than those from random-flight simulations at prediction times less than about 10 hours and essentially equivalent at longer times consistent with theory [*Zambianchi and Griffa*, 1994]. However, it is important to note that the improved effectiveness is simply due to a positive bias in the search area, which, in the SAR problem, dilutes the search effort.

[43] Horizontal dispersion coefficients estimated from fitting the random-flight turbulence model to autocovariance functions of CODAR-drifter differences are in the range of 70–225 m^2/s (Table 2). Higher values are estimated in the NJ shelf region (>140 m^2/s) than in the BI region (<110 m^2/s). We note here that although horizontal dispersion coefficients can be estimated directly using

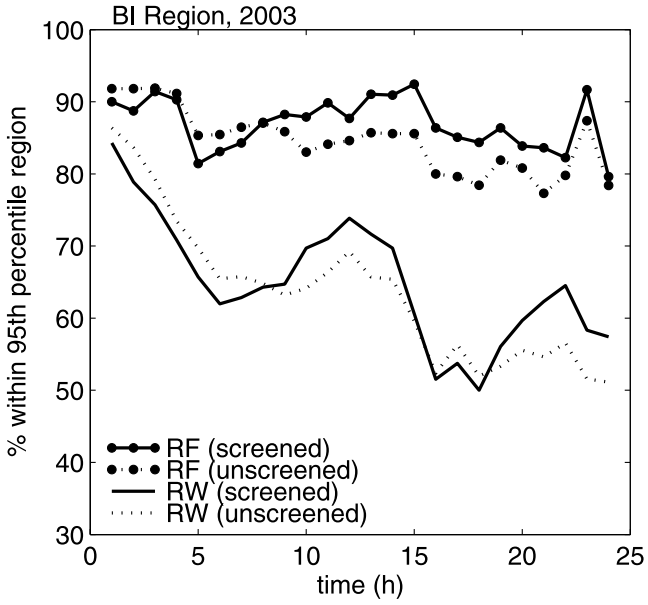

Figure 12. Comparison of the uncertainty bounds for predicted drifter position using the random-flight (lines and circles) and random-walk (lines) turbulence models for the BI region. The solid curves are computed using only those trajectories that both start and end within the 10% coverage zone, while the dotted curves are computed based on all trajectories that start within the nominal coverage zone. For each prediction time we plot the percent of cases where the actual drifter location at that time fell within the estimated 95% confidence region.

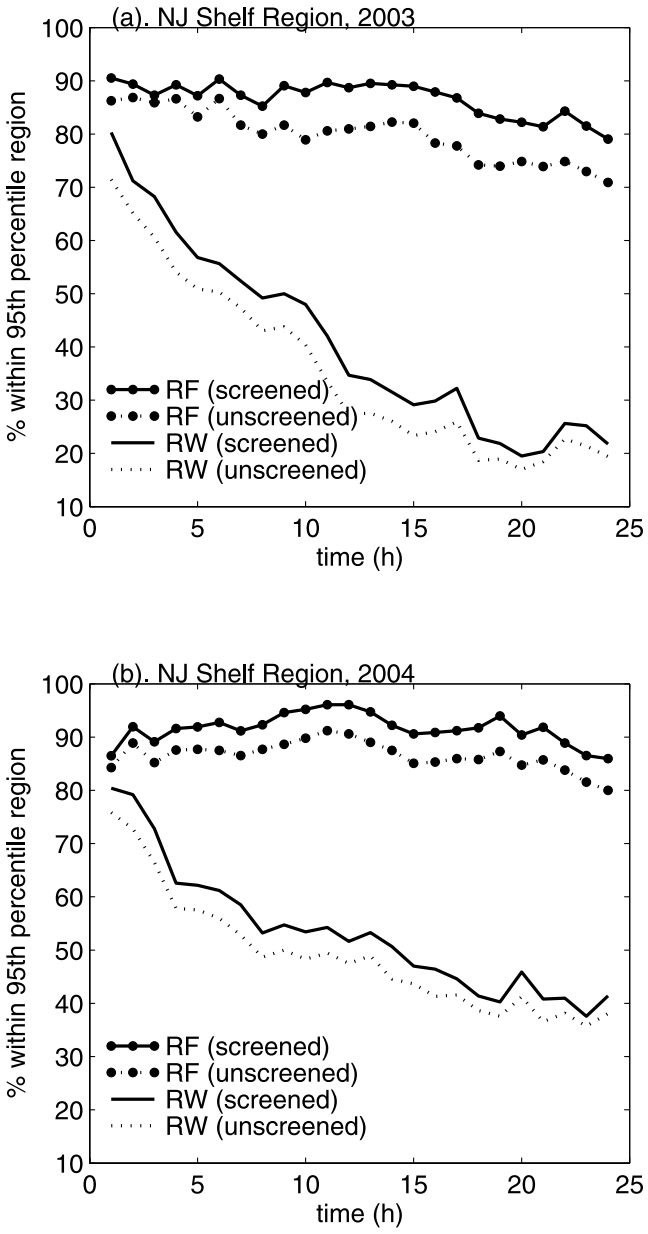

Figure 13. Same as Figure 12 for the NJ shelf region during (a) 2003 and (b) 2004.

drifter tracks from a cluster of drifters, this was not possible here because we did not have enough simultaneous drifter releases to form statistically meaningful clusters. Using *Okubo*'s [1971] empirical formula for the apparent horizontal diffusion as a function of horizontal length scale of diffusion, we compute a diffusion coefficient of $\sim$25 m^2/s using a length scale of 25 km (a typical value of the 95th percentile separation in Figures 8–10). The significantly larger values obtained in this study may result from the fact that the turbulent statistics in Table 2 were computed from time series of velocity difference between drifters and CODAR. The drifter-CODAR differences arise from turbulent motions at scales unresolved by CODAR measurements as well as from errors in the CODAR measurements themselves, including those that arise from differing effective depths between the drifters and CODAR. Thus, the estimated dispersion coefficients may have a large component due to CODAR uncertainties that is unrelated to geophysical turbulence. Consequently, if currents from a numerical model of the circulation were employed instead of the CODAR currents, then the statistics of the differences would be different. However, the approach we have demonstrated would still be applicable.

[44] The turbulent velocity statistics estimated in this study were computed as averages over the region and time period sampled by the drifter ensembles. Comparison of the statistics from the two deployments in the NJ shelf region (Table 2) indicate substantial differences in dispersion between the spring and summer. It is likely that horizontal dispersion is also spatially variable, although the available drifter data are not sufficient to quantify this. Note that comparison of the statistics from the BI region and the NJ shelf region is complicated by the fact that the two regions are observed with CODAR systems using different frequencies with corresponding differences in effective depths.

6. Summary and Conclusions

[45] Comparison of real drifter trajectories and trajectories predicted using CODAR-derived surface currents illustrates the value of these data for search and rescue operations. For prediction times of 1–24 h, the mean (and 95th percentile) distance between the CODAR-predicted position and the real position is smaller than the distance traveled by the drifter. This indicates that predictions using CODAR velocities are more accurate than the so-called "persistence" forecast (zero drifter velocity). Although, not shown here, CODAR trajectory predictions are also superior

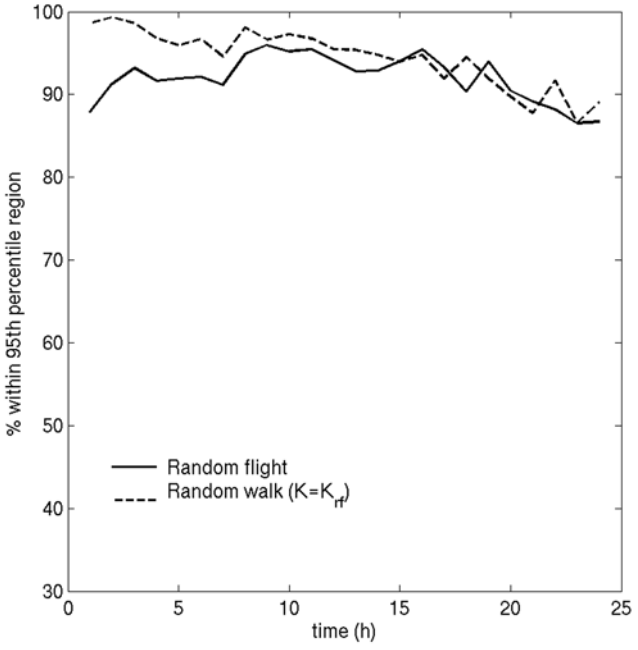

Figure 14. Comparison of the uncertainty bounds for predicted drifter position using the random-flight model (solid) and random-walk model with increased diffusivity (dashed) for the 2004 NJ shelf deployment. The random-walk diffusivity in this case was increased to equal the corresponding random-flight value.

to those produced using present U.S. Coast Guard practice, in which the advective velocity is obtained from NOAA tidal current predictions in nearshore waters and a surface current climatology offshore [*O'Donnell et al.*, 2005].

[46] The statistics of the combination of subgrid-scale velocity and CODAR velocity error that contribute to the dispersion of a cloud of pseudo-drifters have been estimated using the ensemble-averaged covariance functions of CODAR-drifter velocity differences. Approximate consistency of the estimates of turbulent velocity variance and timescale was demonstrated for the random-flight turbulence model by evaluation of the resulting search areas, defined as the region in which 95% of the pseudo-drifters are located. The random-flight search areas include the real drifter location in 80–95% of cases. Using the turbulent velocity variances estimated from the zero-lag autocovariance function, as for the random-flight model, the random-walk search areas were significantly less effective. This is a consequence of the fact that the effective turbulent timescale in the random-walk formulation is one half of the time step used in the integration of the Eulerian velocity, 0.5 hours in this study. One can achieve satisfactory search area predictions using the random-walk model only by specifying a diffusion coefficient that is estimated using a model of turbulence that allows for finite turbulent integral timescales, such as the random-flight model, and inflating the turbulent velocity variance to achieve more rapid dispersion at short times.

[47] This study has demonstrated the value of surface current data derived from HF radar in combination with drifter observations for the practical prediction of particle trajectories in the coastal ocean. The methodology used here for estimating uncertainty regions for predictions does not require the deployment of drifter clusters, from which explicit horizontal diffusivity can be estimated. Instead, velocity observations from an ensemble of drifters passing through the radar domain are used to estimate effective fluctuation statistics that are employed in a stochastic particle model. The method is therefore well suited to the use of "drifters of opportunity" that may be deployed for other purposes but that eventually pass through an HF radar coverage region. The question of how many such drifters are needed to accurately characterize the velocity fluctuation statistics is a question that will require further study.

[48] **Acknowledgments.** Funding for this study was provided by the U.S. Coast Guard Research and Development Center through contract DTCG39-00-D-R00008 to Anteon Corporation. We thank Adam Houk and Hugh Roarty for their efforts in maintaining continuous operation of the CODAR systems and acknowledge the U.S. Coast Guard for their invaluable assistance in the deployment of the drifters. This work would not have been conducted without the effective advocacy of Lew Lewandowski and Sean Lester. We thank Malcolm Spaulding, Eoin Howlett, Paul Hall, Tatsu Isaji, Liz Anderson, Tom McClay, and Grant McCardell for insightful comments on our work and drafts of this report. We also acknowledge the two anonymous reviewers whose comments led to significant improvements of this paper.

References

Allen, A. A. (1996), Performance of GPS/Argos Self-Locating Datum Marker Buoys (SLDMBs), in *Proceedings of Coastal Ocean-Prospects for the 21st Century (Oceans '96)*, pp. 857–861, Mar. Technol. Soc., Columbia, Md.

Brickman, D., and P. C. Smith (2002), Lagrangian stochastic modeling in coastal oceanography, *J. Atmos. Oceanic Technol.*, *19*, 83–99.

Chapman, R. D., and H. C. Graber (1997), Validation of HF radar measurements, *Oceanography*, *10*, 76–79.

Csanady, G. T. (1973), *Turbulent Diffusion in the Environment*, 248 pp., Springer, New York.

Davis, R. E. (1985), Drifter observations of coastal surface currents during CODE: The method and descriptive view, *J. Geophys. Res.*, *90*, 4741–4755.

Griffa, A. (1996), Applications of stochastic particle models to oceanographic problems, in *Stochastic Modelling in Physical Oceanography*, edited by R. J. Adler, P. Müller, and B. L. Rozovskii, Springer, New York.

Griffa, A., K. Owens, L. Piterbarg, and B. Rozovskii (1995), Estimates of turbulence parameters from Lagrangian data using a stochastic particle model, *J. Mar. Res.*, *53*, 371–401.

Gurgel, K. W. (1994), Shipborne measurement of surface current fields by HF radar, *L'Onde Electr.*, *74*, 54–59.

James, M. K., P. R. Armsworth, L. B. Mason, and L. Bode (2002), The structure of reef fish metapopulations: modelling larval dispersal and retention patterns, *Proc. R. Soc. London, Ser. B*, *269*, 2079–2086.

Kenyon, K. E. (1969), Stokes drift for random gravity waves, *J. Geophys. Res.*, *74*, 6991–6994.

Kohut, J. T., H. J. Roarty, and S. M. Glenn (2006), Characterizing observed environmental variability with HF Doppler radar surface current mappers and acoustic Doppler current profilers, *IEEE J. Oceanic Eng.*, in press.

Large, W. G., and S. Pond (1981), Open ocean momentum flux measurements in moderate to strong winds, *J. Phys. Oceanogr.*, *11*, 324–336.

O'Donnell, J., et al. (2005), Integration of Coastal Ocean Dynamics Application Radar (CODAR) and Short-Term Prediction System (STPS) surface current estimates into the Search and Rescue Optimal Planning System (SAROPS), *U.S. Coast Guard Tech. Rep., DTCG39-00-D-R00008/HSCG32-04-J-100052*.

Okubo, A. (1971), Oceanic diffusion diagrams, *Deep Sea Res.*, *18*, 789–802.

Pierson, W. J., and L. Moskowitz (1964), A proposed spectral form for fully developed wind seas based on the similarity theory of S. A. Kitaigorodskii, *J. Geophys. Res.*, *69*, 5181–5190.

Schmidt, R. O. (1986), Multiple emitter location and signal parameter estimation, *IEEE Trans. Antennas Propag.*, *AP-34*, 276–280.

Stewart, R. H., and J. W. Joy (1974), HF radio measurements of surface currents, *Deep Sea Res.*, *21*, 1039–1049.

Thompson, K. R., J. Sheng, P. C. Smith, and L. Cong (2003), Prediction of surface currents and drifter trajectories on the inner Scotian Shelf, *J. Geophys. Res.*, *108*(C9), 3287, doi:10.1029/2001JC001119.

Ullman, D. S., and D. L. Codiga (2004), Seasonal variation of a coastal jet in the Long Island Sound outflow region based on HF radar and Doppler current observations, *J. Geophys. Res.*, *109*, C07S06, doi:10.1029/2002JC001660.

Ullman, D., J. O'Donnell, C. Edwards, T. Fake, D. Morschauser, M. Sprague, A. Allen, and B. Krenzien (2003), Use of Coastal Ocean Dynamics Application Radar (CODAR) technology in U. S. Coast Guard search and rescue planning, *U. S. Coast Guard Rep., CG-D-09-03*.

Zambianchi, E., and A. Griffa (1994), Effects of finite scales of turbulence on dispersion estimates, *J. Mar. Res.*, *52*, 129–148.

A. Allen, U.S. Coast Guard Office of Search and Rescue, Groton, CT 06340, USA.

T. Fake and J. O'Donnell, Department of Marine Sciences, University of Connecticut, Groton, CT 06340, USA.

J. Kohut, Institute of Marine and Coastal Studies, Rutgers University, New Brunswick, NJ 08901, USA.

D. S. Ullman, Graduate School of Oceanography, University of Rhode Island, Narragansett, RI 02882, USA. (d.ullman@gso.uri.edu)